Experimental Cell Research 369 (2018) 251–265

Contents lists available at ScienceDirect

Experimental Cell Research

journal homepage: www.elsevier.com/locate/yexcr

Plakophilin3 loss leads to an increase in lipocalin2 expression, which is required for tumour formation

Srikanta Basu[a,c], Nazia Chaudhary[a,c], Sanket Shah[b,c], Carol Braggs[a], Aakanksha Sawant[a], Simone Vaz[a], Rahul Thorat[a], Sanjay Gupta[b,c], Sorab N. Dalal[a,c,*,1]

[a] Advanced Centre for Treatment Research and Education in Cancer (ACTREC), Tata Memorial Centre, Kharghar Node, Navi Mumbai, Maharashtra, India
[b] Epigenetics and Chromatin Biology Group, Gupta Lab, Cancer Research Institute, Advanced Centre for Treatment, Research and Education in Cancer (ACTREC), Tata Memorial Centre, Kharghar, Navi Mumbai 410210, India
[c] Homi Bhabha National Institute, Training School Complex, Anushakti Nagar, Mumbai 400085, India

ARTICLE INFO

Keywords:
Desmosome
Plakophilin3
Lipocalin2
p38 MAPK

ABSTRACT

An increase in tumour formation and metastasis are observed upon plakophilin3 (PKP3) loss. To identify pathways downstream of PKP3 loss that are required for increased tumour formation, a gene expression analysis was performed, which demonstrated that the expression of lipocalin2 (LCN2) was elevated upon PKP3 loss and this is consistent with expression data from human tumour samples suggesting that PKP3 loss correlates with an increase in LCN2 expression. PKP3 loss leads to an increase in invasion, tumour formation and metastasis and these phenotypes were dependent on the increase in LCN2 expression. The increased LCN2 expression was due to an increase in the activation of p38 MAPK in the HCT116 derived PKP3 knockdown clones as LCN2 expression decreased upon inhibition of p38 MAPK. The phosphorylated active form of p38 MAPK is translocated to the nucleus upon PKP3 loss and is dependent on complex formation between p38 MAPK and PKP3. WT PKP3 inhibits LCN2 reporter activity in PKP3 knockdown cells but a PKP3 mutant that fails to form a complex with p38 MAPK cannot suppress LCN2 promoter activity. Further, LCN2 expression is decreased upon loss of p38β, but not p38α, in the PKP3 knockdown cells. These results suggest that PKP3 loss leads to an increase in the nuclear translocation of p38 MAPK and p38β MAPK is required for the increase in LCN2 expression.

1. Introduction

Desmosomes are cell-cell adhesion junctions that anchor intermediate filaments thus forming a tissue wide intermediate filament network maintaining tissue integrity and homeostasis [1,2]. Three major protein families contribute to desmosome assembly, the desmosomal cadherins (desmogleins and desmocollins), the plakin family (desmoplakin) and the ARM repeat containing proteins (plakoglobin and plakophilins (PKP)) [1,2]. Of the three PKP isoforms present in humans [3], only PKP3 is ubiquitously expressed in most epithelial tissues. PKP3 forms a complex with a broad repertoire of desmosomal proteins [4] and is found in both nuclear and cytoplasmic fractions suggesting that the regulation of PKP3 localization may determine the dynamics of desmosome formation and contribute to other PKP3 functions [5].

A decrease in PKP3 expression has been associated with tumour progression in multiple tumour types [6–10]. PKP3 loss leads to an increase in cell migration, invasion and colony formation in soft agar in vitro and increased tumour formation and metastasis in vivo [11]. A microarray analysis demonstrated that the expression of MMP7 and Lipocalin2 (LCN2) increased upon PKP3 loss in multiple cell lines [12]. The increase in MMP7 expression was dependent on the activity of the phosphatase of regenerating liver (PRL-3) [12]. The increase in PRL-3 activity is also required for an increase in the levels of keratin8 (K8) in these cells and both MMP7 and K8 are required for the transformation observed upon PKP3 loss [12,13].

LCN2, also known as NGAL (neutrophil gelatinase associated lipocalin), is a secreted glycoprotein [14,15] and is required to maintain the integrity of the gastro-intestinal mucosa [16]. LCN2 is over-expressed in multiple tumour types [14,17]. An increase in LCN2 expression was observed in colorectal carcinomas in clinical studies and is an indicator of colon cancer progression from adenoma to carcinoma [18–20]. LCN2 over-expression leads to increased tumour formation in xenograft colon cancer models suggesting that LCN2 over-expression drives tumour progression in the colon [19].

This report demonstrates that LCN2 is required for the increase in

* Corresponding author at: Advanced Centre for Treatment Research and Education in Cancer (ACTREC), Tata Memorial Centre, Kharghar Node, Navi Mumbai, Maharashtra, India.
E-mail address: sdalal@actrec.gov.in (S.N. Dalal).
[1] <http://www.actrec.gov.in/pi-webpages/SorabDalal-2017/sorab-index-2017.html>.

https://doi.org/10.1016/j.yexcr.2018.05.026
Received 12 December 2017; Received in revised form 22 May 2018; Accepted 23 May 2018
Available online 24 May 2018
0014-4827/

neoplastic transformation and tumour formation observed upon PKP3 loss. The increase in LCN2 expression upon PKP3 loss was dependent on an increase in the activity of p38 MAPK and suggest that PKP3 loss leads to the activation of multiple pathways required for tumour progression and metastasis.

2. Materials and methods

2.1. Plasmids and constructs

The oligonucleotides used to generate the LCN2, p38α and p38β shRNA constructs (Table S1) were cloned downstream of the U6 promoter in pLKO.1-EGFPf-puro [21]. Overlapping fragments of the LCN2 promoter were cloned into the MCS of pGL3 (Promega) digested with *Kpn*I and *Xho*I. The sequences of the oligonucleotides used for cloning these promoter fragments are in Table S2. pRL-TK (Promega) was used as a transfection control. The GST tagged, Myc tagged wild type (WT) PKP3 and PKP3 deletion mutants have been described previously [22] The shRNA resistant Ds Red tagged WT PKP3 and the N terminal deletion mutant (51-797, 101-797 and 151-797) plasmids have been described previously [22].

2.2. Cell culture and transfections

HCT116, HaCaT and FBM [23] derived vector control and PKP3 knockdown cells were cultured as previously described [11,13,22]. The PKP3 LCN2 double knockdown cell lines were generated by transfecting the PKP3 knockdown clone, shpkp3-2 with the pLKO.1 EGFP-f-puro vector expressing an shRNA targeting LCN2 using Lipofectamine LTX reagent (Life Technologies). The cells were maintained in media containing 5 μg/ml blasticidin and 0.5 μg/ml puromycin to obtain single cell clones. Similarly, double knockdown clones derived from shpkp3-2 for p38α MAPK and p38β MAPK were generated using shRNAs targeted against p38α MAPK and p38β MAPK. Lipofectamine LTX reagent (Life Technologies) was also used for transient transfection of the plKO.1 EGFP-f-puro vector expressing the shRNAs targeting p38β MAPK and also for transfection of the plKO.1 EGFP-f-puro empty vector in the PKP3 knockdown clone shpkp3-2. To assay the contribution of p38 MAPK to LCN2 expression, the p38 MAPK inhibitor SB203580 (catalogue number 8307, Sigma) was added to cells at a concentration of 1 μM for 24 h. The MEK1/2 inhibitor, PD 98059 (catalogue number P215, Sigma) was added to the cells at a concentration of 50 μM and 100 μM as indicated. These high concentrations were used as the experiments were performed in the presence of serum as serum withdrawal led to an increase in LCN2 levels [24–26]. To determine if reintroduction of PKP3 leads to a decrease in LCN2 levels and a decrease in p38MAPK activation, the PKP3 knockdown clones were transfected with either the vector control or a previously described shRNA resistant PKP3 construct [22]. 72 h post selection in puromycin, protein extracts were prepared and analysed by Western blot.

2.3. Isolation of total RNA, real time PCR reactions and reverse transcriptase coupled PCR reactions

The forward and reverse oligonucleotides used in this study are shown in Table S3. Quantitative and semi-quantitative reverse transcriptase PCRs were performed as described [12].

2.4. Antibodies and Western blot analysis

Protein extracts were prepared as described previously [12,27]. Protein extracts were prepared either in EBC lysis buffer (120 mM NaCl, 50 mM Tris-HCL (pH 8), 0.5% NP40 and protease inhibitors [5 μg/ml leupeptin, 10 μg/ml aprotinin, 0.2 mM sodium orthovanadate and 100 mM sodium fluoride]) [27] or in 1× sample buffer as described [12]. Acetone precipitation of cell supernatants and Western blots were performed as described [12]. Antibody dilutions are shown in Table S4. The blots were developed using Supersignal West Pico Chemiluminescent Substrate (Pierce), Super Signal West Femto Chemiluminescent Substrate (Pierce) and Clarity Western ECL substrate (Bio-rad) as per the manufacturer's instructions.

2.5. Scratch wound healing assays, matrigel invasion assays and soft agar colony formation assays

Scratch wound healing assays and matrigel invasion assays were performed as described [12]. The results shown are an average of three independent experiments.

2.6. Growth curves

The effect of LCN2 knockdown on cell proliferation of the HCT116 derived PKP3 knockdown clones was analysed by performing growth curves as described [11].

2.7. Luciferase reporter assays

Luciferase reporter assays were performed using the Dual Luciferase reporter assay system (Promega) as per the manufacturer's instructions.

2.8. Tumour formation in nude mice

BALB/c Nude mice (CAnN.Cg-*Foxn1nu*/Crl) of 6–8 weeks old, provided by the ACTREC animal house facility, were used for the study. 1×10^6 cells of the HCT116 based shpkp3-2 derived vector control and double knockdown clones were re-suspended in 100 μl of PBS and injected sub-cutaneously in the dorsal flank of mice. Six mice were injected for each clone. Tumour formation was monitored at intervals of 2–3 days and tumour size was calculated weekly for 5 weeks using the formula ($0.5 \times LV^2$) where L is the largest dimension and V its perpendicular dimension [11,12]. The maximum tumour volume of 1045.421 mm^3 was obtained 5th week post-injection for a mouse injected with shpkp3-2-vec.

2.9. Ethics statement

Animals were maintained in the ACTREC animal house facility following the national guidelines mentioned by the Committee for the Purpose of Control and Supervision of the Experiments on Animals (CPCSEA), Ministry of Environment, Forest and Climate Change, Government of India. A controlled environment was provided to the animals with a temperature of 22 ± 2 °C and relative humidity maintained at 40–70%. A 12 h′ day night cycle was maintained (7:00–19:00 day and 19:00–7:00 night). The animals were given autoclaved balanced diet prepared in house and sterile water. Individually ventilated Cage system (IVC, M/S Citizen, India) was used to house mice used in the experiments. These IVCs were provided with autoclaved corn cob as bedding for the mice. Animal euthanasia was done under the guidelines of AVMA as mentioned above using CPCSEA recommended euthanizing agent, carbon dioxide. The Institutional Animal Ethics Committee (IAEC) of the Advanced Centre for Treatment Research and Education in Cancer (ACTREC) approved all the protocols used in this report. The project number for the study is 16/2008 and was approved in November 2008.

2.10. Immunofluorescence assays

Immunofluorescence analysis was performed as described previously [11,22]. Cells were cultured on glass coverslips at 50–70% confluency. The cells were washed carefully twice with 1× PBS followed by fixation in 4% formaldehyde for 20 min at room temperature. The cells were then washed thrice with PBS and cell permeabilization

was performed using 0.3% Triton-X100 in 1× PBS for 20 min at room temperature. Primary antibodies, p38 MAPK (1:50 dilution) was prepared in 3% BSA in 1× PBS + 0.1% NP-40 solution. The cells were incubated with the primary antibody solution for 16 h at 4 °C. The cells were then washed four times alternatively with 1× PBS and 1× PBS + 0.1% NP-40. Secondary antibodies were prepared in 3% BSA in 1× PBS + 0.1% NP-40 solution. The secondary antibody, Alexa 488 conjugated anti rabbit IgG (Invitrogen) was used at a dilution of 1:100 and incubated for 30 min at room temperature in a humidifying container. The cells were washed six times alternatively with 1× PBS and 1× PBS + 0.1% NP-40. Thereafter, 50 µl of DAPI (2.5 µg/ml) was added to the cells and incubated for exactly 5 min at room temperature. The cells were washed four times with 1× PBS. The coverslips were then mounted on chromic acid treated, clean glass slides using 10–20 µl of Vectashield mounting agent (Vector Laboratories). Confocal images were obtained by using a LSM 510 Meta Carl Zeiss Confocal system with an Argon 488 nm and Helium/Neon 543 nm lasers or an LSM780 Carl Zeiss Confocal system with an Argon 488 nm and Helium/Neon 561 nm lasers. Line scans were drawn across the longest length of 30 random cells in three independent experiments using ImageJ software. The plot profile function of ImageJ was used to determine the distribution of signal intensities of p38 MAPK and DAPI along these line scans. The signal intensity values were compiled and the average intensity was plotted against the distance (µm) from the start to the end point of the line scans.

The intensity of staining for p38 MAPK in the nucleus and the total cell were measured using the ImageJ software. The nucleus of cells was marked using the region of interest (ROI) tool and the signal intensity of immunofluorescence from the nucleus was determined. The area of the nucleus was used for normalization. Similarly, the signal intensity of immunofluorescence from the total cell was determined and normalized to the area of the total cell. Cytoplasmic mean intensity was calculated using the formula: ((mean intensity of total p38 × total area of cell) − (mean intensity of nuclear p38 × area of the nucleus)). Thereafter, the ratio of the nuclear/cytoplasm mean signal intensities of p38MAPK were determined and plotted using graph pad prism software.

2.11. Cytoplasmic and nuclear fractionation assays

Nuclear and cytoplasmic fractions were isolated from HCT116 derived PKP3 knockdown clones and the vector control clone using the NE-PER kit (PROMEGA). Equal protein amounts of the total cell, cytoplasmic and nuclear extracts were resolved on SDS-PAGE gels followed by Western blot analysis. The total cell lysates obtained from the above cell lines served as controls. Western blots from three independent experiments were analysed on a Bio-Rad ChemiDoc Imaging System and luminescence intensity quantitated using Image Lab software. The intensity of each individual p38 or p-p38 MAPK band was analysed using the automated “lane and bands” analysis tool and the intensity of the cytoplasmic fractions normalized to α-tubulin and the nuclear fraction to Lamin-A. The relative intensity of p-p38 MAPK and p38 MAPK have been plotted. Where indicated the p value was calculated using a student's *t*-test (* indicates p value < 0.01).

2.12. GST pulldown assays and Immunoprecipitation assays

Pulldown assays with GST tagged WT or deletion mutants of PKP3 were performed as described [22]. Immunoprecipitation experiments were performed using Myc tagged WT PKP3 and sequential N terminal deletion mutants of PKP3. 48 h′ post transfection, the cell culture medium was decanted from both the plates. 1 ml of cold PBS (pre-cooled to 4 °C) was added to each plate and using a cell scraper, the cells were scraped and the cells lysed in 1 ml of EBC lysis buffer containing protease and phosphatase inhibitors (Leupeptin 10 µg/ml, Aprotinin 20 µg/ml, Sodium Fluoride 50 mM, Sodium orthovanadate 1 mM, EDTA 1 mM, Pepstatin A 10 µg/ml and PMSF 1 mM). The extract was incubated with the following primary antibodies ((Myc antibody (1:100), p38α antibody (dilution 1:100) or p38β antibody (dilution 1:100)) for two hours at 4 °C, followed by addition of 30 µl of a 50% slurry of Protein G Sepharose (GE Healthcare) and an additional incubation at 4 °C for one hour. The reaction mixtures and 5% of the whole cell extracts were resolved on SDS-PAGE gels followed by Western blotting with the appropriate antibodies.

2.13. In silico analysis of LCN2 and PKP3 expression in microarray dataset and their inter-correlation

To analyze the expression levels of LCN2 and PKP3 mRNAs in colon cancer, gene expression profiling data sets were obtained from the National Center for Biotechnology Information (NCBI) Gene Expression Omnibus (GEO) database (Accession no. GSE39582) as it was the only dataset that had both normal (19) and tumour (443) samples. Raw data (CEL files) were downloaded from GEO and the Affymetrix® Expression Console™ Software (Version 1.3) was used to generate.txt files for further processing. All subsequent data analyses were performed in R 3.3.3 (http://www.R-project.org/). The Limma package (Smyth, 2004) was used for background adjustment, summarization and quantile normalization. Normalization was made using the Robust Multichip Average (RMA) pre-normalization algorithm (RA, 2003). After normalization, the values were log2 transformed and scatter boxplots were created for LCN2 and PKP3 genes for both normal and tumour samples. P values were calculated using *t*-test and values < 0.05 were considered to be statistically significant. Z scores for each tumour sample was calculated by subtracting the log2 normalized values of each tumour sample from average mean log2 normalized value of normal samples and dividing that result by the SD of log2 normalized values of the normal samples. Heat map was also constructed using R 3.3.3 where z-score > 1.5 was considered as up-regulation and < -1.5 was considered as down-regulation.

2.13.1. Expression of p38 target genes in PKP3 knockdown cells

Using a previously published list of validated p38 transcriptional targets [28], we have examined the expression of these genes in our microarray data set. The raw data was processed as described earlier in materials and methods and the log2 normalized signal intensity values were used to generate a heatmap.

3. Results

3.1. LCN2 is required for the tumour progression observed upon PKP3 loss

Semi-quantitative RT-PCR (Fig. 1A), quantitative RT-PCR (qRT-PCR) (Fig. 1B) and Western blot assays (Fig. 1C) demonstrated that LCN2 mRNA and protein increased in the PKP3 knockdown cells as compared to the vector controls in HaCaT, HCT116 and FBM cells. To determine if the increase in LCN2 levels contributed to the increase in transformation observed upon PKP3 loss [11], LCN2 expression was inhibited in the PKP3 knockdown clone shpkp3-2 using vector driven RNA interference. Four LCN2 + PKP3 double knockdown clones were generated using the shRNAs X (shpkp3-2-shlcn2-1 and shpkp3-2-shlcn2-2) and Y (shpkp3-2-shlcn2-3 and shpkp3-2-shlcn2-4). The clone shpkp3-2-vec served as a vector control. Real time PCR assays (Fig. 1D) and Western blot analysis (Fig. S1A) demonstrated that LCN2 mRNA and protein levels were decreased in the double knockdown clones. Cell proliferation assays demonstrated that although PKP3 knockdown clones have a higher rate of cell proliferation as compared to their vector control clones [11], LCN2 loss does not decrease cell proliferation (Fig. S1B) in the HCT116 derived PKP3 knockdown clones. Scratch wound healing assays and trans-well invasion assays demonstrated that loss of LCN2 resulted in a decrease in cell migration and invasion in the PKP3 knockdown cells (Figs. 1E–F and S1C–D).

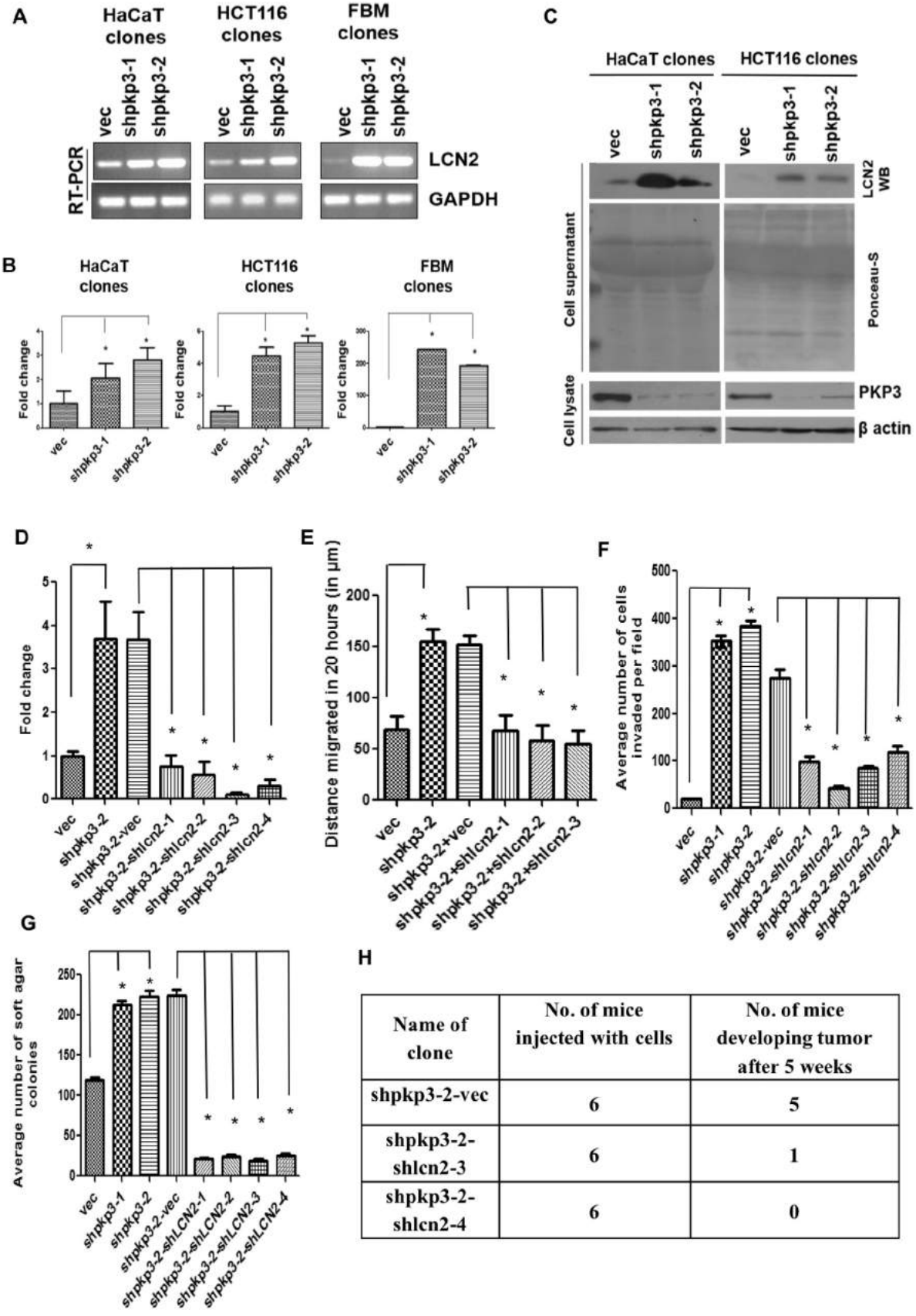

H

Name of clone	No. of mice injected with cells	No. of mice developing tumor after 5 weeks
shpkp3-2-vec	6	5
shpkp3-2-shlcn2-3	6	1
shpkp3-2-shlcn2-4	6	0

(caption on next page)

Fig. 1. PKP3 loss leads to an increase in the expression of LCN2. (A) Semi-quantitative (sq) RT-PCRs were performed using oligonucleotides specific for LCN2 and GAPDH in HaCaT, HCT116 and FBM derived PKP3 knockdown clones and the respective vector controls. The levels of GAPDH serve as a loading control. **(B)** Real time PCR was performed using oligonucleotides specific to LCN2 and GAPDH, with cDNA obtained from the vector control and PKP3 knockdown clones derived from the indicated cell line. Expression of GAPDH has been used for normalization. The fold change in LCN2 mRNA was measured and mean values and standard errors are plotted. **(C)** 300 μg of acetone precipitated cell supernatants or 75 μg of protein extracts were obtained from the HaCaT and HCT116 derived PKP3 knockdown and vector control clones were resolved on 12% SDS PAGE gels followed by Western blotting with antibodies specific to LCN2. The same blot was stained with Ponceau to serve as a loading control. Whole cell extracts were resolved on 12% SDS PAGE gels followed by Western blotting with antibodies specific to PKP3. Western blots for β actin served as a loading control. **(D)** mRNA prepared from the HCT116 derived vector controls (vec) and the PKP3 knockdown clone (shpkp3-2) and the shpkp3-2 derived vector control (shpkp3-2 + vec) and shpkp3-2 derived LCN2 knockdown clones (shpkp3-2 + shlcn2-1, shpkp3-2 + shlcn2-2, shpkp3-2 + shlcn2-3 and shpkp3-2 + shlcn2-4) was used as a substrate for reverse transcriptase followed by real time PCR reactions using oligonucleotides specific for LCN2. GAPDH levels were used for normalization. The fold change in LCN2 mRNA was measured and the mean and standard error plotted. **(E)** Scratch wound healing assays were performed on the HCT116 derived vector control (vec), PKP3 knockdown clone (shpkp3-2), shpkp3-2 derived vector control clone (shpkp3-2-vec) and shpkp3-2 derived LCN2 knockdown clones (shpkp3-2 + shlcn2-1, shpkp3-2 + shlcn2-2 and shpkp3-2 + shlcn2-3) and the distance migrated plotted. The mean and standard error for three independent experiments is plotted. **(F)** Matrigel invasion assays were performed in Boyden's chambers for HCT116 derived vector control cells, PKP3 knockdown clones and the PKP3 and LCN2 double knockdown clones. The number of cells observed in ten random fields of the membrane for each clone was determined as described in Materials and Methods. The mean and standard deviation of three independent experiments is plotted. **(G)** Soft agar colony formation assays were performed with the HCT116 derived vector control and pkp3 knockdown clones, the shpkp3-2 derived double knockdown clones and the shpkp3-2 derived vector control clone. The mean and standard deviation of three independent experiments is plotted. **(H)** 1×10^6 cells of the shpkp3-2 derived vector control or double knockdown clones were injected sub-cutaneously into nude mice and allowed to develop tumours. The table shows the number of mice injected with the respective clones and the number of mice which developed tumours. Wherever indicated the p value was calculated using a student's *t*-test (* indicates a p value < 0.01).

A decrease in expression of LCN2 in the PKP3 knockdown clones led to a decrease in anchorage independent growth (Figs. 1G and S1E) and tumour formation in nude mice (Figs. 1H and S1F). Five of the six mice injected with the vector control developed large tumours. In contrast, only one out of six mice injected with shpkp3-2 + shLCN2-3 developed a tumour at the site of injection and none of the six mice injected with shpkp3-2 + shLCN2-4 developed tumours. These results suggest that the increase in LCN2 expression is required for the enhanced tumour formation observed upon PKP3 loss.

Previous reports had independently demonstrated that a decrease in PKP3 expression [6] and an increase in LCN2 expression [19,20] is observed in colon tumour samples. To determine if the two were related, we first analysed LCN2 and PKP3 expression in a microarray dataset (GSE39582) that contained both normal (19) and tumour samples (566). LCN2 expression is significantly increased and PKP3 expression is significantly decreased in tumour samples as compared to the normal controls (Fig. S2A). Z scores were calculated for LCN2 and PKP3 tumour samples from normalized log2 transformed values (Materials and methods). PKP3 z-scores were sorted from low to high expression and the expression of LCN2 determined in samples with PKP3 low expression (Fig. S2B). The data suggested that 59.57% (112/188) tumour samples had increased expression of LCN2, 19.15% (36/188) tumour samples showed a decrease expression of LCN2 and 21.27% (40/188) patients showed unaltered expression of LCN2 in tumour samples where PKP3 expression was low. These data demonstrate an inverse correlation between LCN2 and PKP3 expression in a majority of colon tumour samples. These results when taken together with the data from IHC studies [6,19,20], suggest that PKP3 loss might lead to increased tumour progression due to a concomitant increase in LCN2 expression.

3.2. MAPK activation is required for the increased LCN2 expression observed upon PKP3 loss

As previous reports have suggested that the activation of p38 MAPK and ERK1/2 signalling stimulate LCN2 expression [29,30], the levels of active p38 MAPK and ERK1/2 were determined in the vector control and PKP3 knockdown clones by Western blotting [31,32]. These experiments demonstrated that PKP3 loss in HCT116 cells results in increased p38 MAPK phosphorylation (Fig. 2A) but not ERK1/2 activation (Fig. 2B). This is consistent with earlier reports suggesting that a disruption of desmosome organization leads to p38 activation [33–35]. p38MAPK activation leads to an increase in expression of multiple genes [28]. To determine if expression of these previously identified target genes was altered upon PKP3 loss, we analysed our microarray data [12] to determine their expression in the PKP3 knockdown clones as compared to the vector control. Log2 normalized intensity values of p38 target genes were plotted as shown in Fig. S2D. These data suggested that upon PKP3 knockdown leads to an increase in the expression of p38 target genes presumably due to increased activation of p38.

To determine if p38 activation is required for LCN2 expression, HCT116 derived PKP3 knockdown and vector control clones were treated with 1 μM SB203580, an inhibitor specific for p38α/β MAPK [36,37]. Inhibition of p38 MAPK activity resulted in a decrease in LCN2 mRNA and protein levels in the PKP3 knockdown clones but not in the vector control (Fig. 2C–D). In contrast, the expression of MMP7, whose expression is also increased upon PKP3 loss [12], remains unaltered upon treatment with the p38 MAPK inhibitor (Fig. S3A) suggesting that p38 MAPK is specifically required for the increase in LCN2 expression observed upon PKP3 loss in HCT116 cells. To determine whether the increase in p38 MAPK activity and LCN2 expression was due to PKP3 loss, shpkp3-1 was transfected with the shRNA resistant DsRed tagged PKP3 or the vector control. Expression of the shRNA resistant PKP3 resulted in a decrease of the active p38 MAPK, which was accompanied by a concomitant decrease in LCN2 levels (Fig. 2E and F), demonstrating that PKP3 loss in HCT116 cells results in the activation of p38 MAPK and an increase in LCN2 expression.

As phosphorylation of p38 MAPK stimulates the translocation of p38 MAPK into the nucleus [38], cellular fractionation assays were performed to determine the localization of p38 MAPK in the HCT116 derived PKP3 knockdown clones and the vector control clone. PKP3 loss resulted in a significant increase in the nuclear localization of p38 MAPK (Fig. 2G and H), with the active p38MAPK being enriched in the nuclear fraction in the PKP3 knockdown cells. Immuno-fluorescence assays were also performed to determine the localization of p38 MAPK in the HCT116 derived PKP3 knockdown clones and the vector control clone. An increase in the nuclear localization of p38 MAPK was detected in the PKP3 knockdown clones (Fig. 3A). Plot profiles of straight lines drawn across the longest length of the cells showed a pan-cellular distribution of p38 MAPK in the vector control cells while in the HCT116 derived PKP3 knockdown clones, the signal intensity of p38 MAPK was higher in the nucleus as compared to the cytoplasm (Fig. 3B). The nuclear to cytoplasmic ratio of the p38 MAPK signal intensity was also higher in the HCT116 derived PKP3 knockdown clones (Fig. 3C).

3.3. PKP3 binds to p38 MAPK and inhibits nuclear translocation of p38 MAPK

To determine if PKP3 forms a complex with p38 MAPK, GST

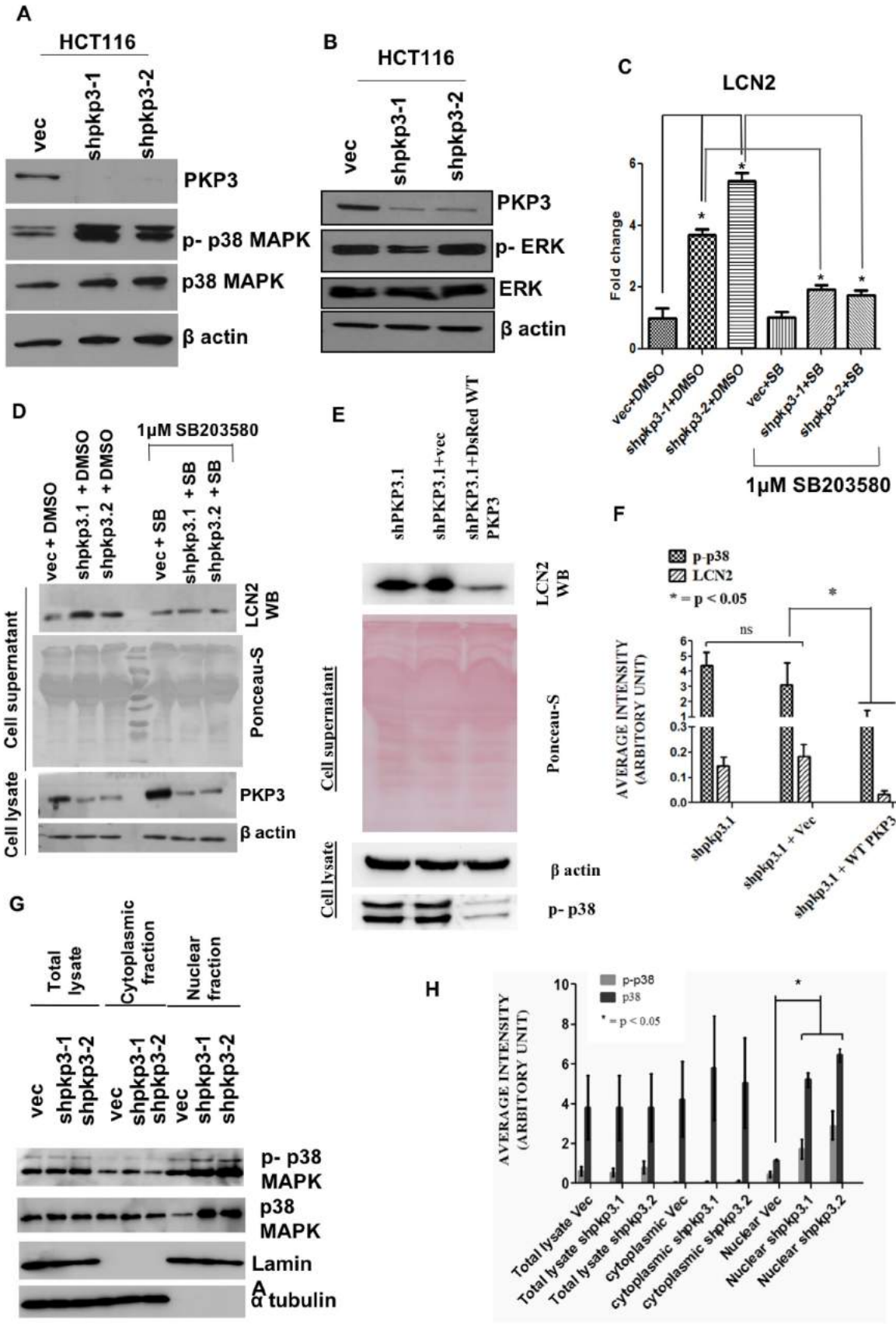

(caption on next page)

Fig. 2. Activation of p38 MAPK leads to an increase in LCN2 expression upon PKP3 loss. (A–B) 75 μg of a whole cell extract (WCE) was resolved on 10% SDS PAGE gels followed by Western blotting with the indicated antibodies. Western blots for β actin served as a loading control. Note that PKP3 levels are lower in PKP3 knockdown clones and p38 MAPK phosphorylation increases but ERK1/2 phosphorylation remains the same in HCT116 cells upon PKP3 loss. **(C)** Real time PCR for LCN2 was performed using cDNA obtained from vector control and HCT116 derived PKP3 knockdown clones after treatment with 10 μM SB203580 (p38 MAPK inhibitor) or DMSO (solvent control) for 24 h. Expression of GAPDH has been used for normalization. The fold change is graphed on the Y-axis and the clone name is on the X-axis. The mean and standard errors are plotted. **(D)** The HCT116 derived PKP3 knockdown and vector control clones were treated with either the p38MAPK inhibitor SB203580 (10 μM) or the vector control, DMSO. 300 μg of acetone precipitated cell supernatants or 100 μg of protein extracts were resolved on 12% SDS PAGE gels followed by Western blotting with antibodies to LCN2. The same blot was stained with Ponceau to serve as a loading control. Whole cell extracts were resolved on 12% SDS PAGE gels followed by Western blotting with antibodies to PKP3. Western blots for β actin served as a loading control. **(E)** Ds-Red tagged shRNA resistant WT PKP3 or vector control plasmid were transiently transfected in the PKP3 knockdown clone, shpkp3-1. After 48 h, post transfection, the cell supernatants were collected and the proteins precipitated with acetone. The cells from the same plates were harvested and lysed to generate protein extracts. 300 μg of acetone precipitated cell supernatants or 100 μg of protein extracts were resolved on 12% SDS PAGE gels followed by Western blotting with the indicated antibodies. A Ponceau stain served as a loading control for the supernatants while Western blots for β actin served as a loading control for the whole cell extracts. (F) Western blots from three independent experiments were analysed on a Bio-Rad ChemiDoc Imaging System and luminescence intensity quantitated using Image Lab software. The intensity of each individual p-p38 MAPK or LCN2 band was analysed using the automated "lane and bands" analysis tool and the intensities were normalized to β actin and Ponceau-S respectively. The relative intensity of p-p38 MAPK and LCN2 have been plotted. Where indicated the p value was calculated using a student's *t*-test (* indicates p value < 0.01). **(G)** 100 μg of total cell lysate, cytoplasmic extract and nuclear extract were resolved on 12% SDS PAGE gels followed by Western blotting with antibodies specific to PKP3, p38 MAPK, phospho-p38 MAPK, Lamin A (marker for nuclear fractions) and α-tubulin (marker for cytoplasmic fractions). Note that p38 MAPK and phospho-p38 MAPK levels in the nuclear fractions are higher in the PKP3 knockdown clones as compared to the vector control clone. (H) 100 μg of total cell lysate, cytoplasmic extract and nuclear extract were resolved on 12% SDS PAGE gels followed by Western blotting with antibodies specific to PKP3, p38 MAPK, phospho-p38 MAPK, Lamin A (marker for nuclear fractions) and α-tubulin (marker for cytoplasmic fractions). Western blots from three independent experiments were analysed on a Bio-Rad ChemiDoc Imaging System and luminescence intensity quantitated using Image Lab software. The intensity of each individual p38 or p-p38 MAPK band was analysed using the automated "lane and bands" analysis tool and the intensity of the cytoplasmic fractions normalized to α-tubulin and the nuclear fraction to Lamin-A. The relative intensity of p-p38 MAPK and p38 MAPK have been plotted. Where indicated, the p value was calculated using a student's *t*-test (* indicates p value < 0.01).

pulldown assays with GST tagged wild type (WT) PKP3 and PKP3 deletion mutants were performed. These experiments demonstrated that PKP3 associates with p38 MAPK and the N terminal domain of PKP3 is required for the association of PKP3 and p38 MAPK (Fig. 4A–B). Immuno-precipitation experiments using MYC tagged WT PKP3 and N terminal deletion mutants of PKP3 (51-797, 101-797 and 151-797) [22], demonstrated that the region between amino acids 101-150 in PKP3 is required for association with p38 MAPK (Fig. 4C–D).

To determine if the association of PKP3 with p38 MAPK can inhibit the nuclear translocation of p38 MAPK observed in the PKP3 knockdown cells, the HCT116 derived PKP3 knockdown clone shpkp3-1 was transfected with the shRNA resistant DsRed tagged WT PKP3 and the N terminal deletion mutants (51-797, 101-797 and 151-797) followed by immunofluorescence assays to determine the localization of p38 MAPK. Loss of PKP3 led to an increase in the levels of p38 in the nucleus as determined by measuring the nuclear to cytoplasmic ration for p38 (Fig. 5A and B). Expression of WT PKP3 or PKP3 mutants that bound to p38 resulted in a decrease in the nuclear localization of p38 MAPK. In contrast, in cells expressing the p38 MAPK binding deficient mutant, 151-797, p38 nuclear localization was unaltered (Fig. 5A and B). Thus, PKP3 might inhibit the nuclear translocation of p38 MAPK and loss of PKP3 leads to p38 MAPK activation, nuclear localization and an increase in LCN2 expression.

3.4. Association of PKP3 with p38 MAPK is important for the increase in LCN2 transcription

To determine if PKP3 loss led to an increase in LCN2 transcription, three overlapping regions of the LCN2 promoter [39,40] containing promoter regions − 1138 to + 64, − 417 to + 64 and − 153 to + 64 (named L1, L2 and L3 respectively) (Fig. 6A) were cloned upstream of a luciferase reporter. A vector expressing a Renilla luciferase reporter gene served as an internal control [41,42]. The promoter activity of the L1 fragment was higher in the PKP3 knockdown clones as compared to the vector control cells. No difference in activity was observed for the L2 and L3 fragments in the vector control v/s the PKP3 knockdown cells (Fig. 6B). Therefore, the region between − 1138 and − 417 bps of the LCN2 promoter might contain enhancer elements required for the increase in transcription observed upon PKP3 loss.

To determine if the association of PKP3 with p38 MAPK is important for regulation of LCN2 expression, HCT116 derived PKP3 knockdown clones and the vector control clones were transfected with the L1 promoter fragment in the presence of shRNA resistant DsRed WT PKP3 or the N terminal deletion mutants (51-797, 101-797 and 151-797). Luciferase reporter assays were performed to determine changes in activity of the LCN2 promoter. The luciferase reporter assay demonstrated that, re-expression of WT PKP3 and the 51-797or 101-797 mutants resulted in a decrease in the activity of the LCN2 promoter. In contrast, expression of the PKP3 mutant 51-797, which does not form a complex with p38 MAPK, did not suppress LCN2 promoter activity (Fig. 6C). As controls, promoter activity of the L1 fragment was demonstrated to be increased in the PKP3 knockdown clone, shpkp3-1, as compared to the vector control clone (Fig. 6C).

3.5. p38β MAPK but not p38α MAPK is required for the increased expression of LCN2 upon PKP3 loss

Four isoforms of p38 MAPK exist in mammalian cells [43] and SB203580 specifically inhibits p38α and p38β [36,37]. Immunoprecipitation assays with antibodies to p38α or p38β demonstrated that PKP3 could form a complex with both p38α and p38β MAPK (Fig. 7A–B). To determine whether p38α or p38β or both were required for the increase in LCN2 expression upon PKP3 loss, their expression was inhibited in the PKP3 knockdown clone shpkp3-2 using vector driven RNA interference. Three p38α MAPK + PKP3 double knockdown clones were generated using the shRNAs p38α1 (shpkp3-2-shp38α1.2) and p38α2 (shpkp3-2-shp38α2.2 and shpkp3-2-shp38α2.4). Four p38β MAPK + PKP3 double knockdown clones were generated using the shRNAs p38β1 (shpkp3-2-shp38β1.1 and shpkp3-2-shp38β1.4) and p38β2 (shpkp3-2-shp38β2.4 and shpkp3-2-shp38β2.5). The clone shpkp3-2-vec served as a vector control. The expression of p38α and p38β MAPKs in the HCT116 derived vector control, PKP3 knockdown clones and p38α or p38β double knockdown clones were validated by qRT-PCR (Fig. 7C–D) and Western blotting (Fig. 7E). These experiments demonstrated that the knockdowns were specific. A qRT-PCR analysis demonstrated that LCN2 expression increased upon PKP3 loss in HCT116 cells while loss of p38α resulted in a further increase in LCN2 expression (Fig. 7F). Western blotting of cell supernatants showed that no increase in extracellular LCN2 levels upon p38α loss despite the increase in mRNA levels (Fig. S3B). In contrast, p38β loss led to a decrease in LCN2 expression observed upon PKP3 loss as observed both by qRT-PCR analysis (Fig. 7F) and by Western blotting (Fig. S3C). These

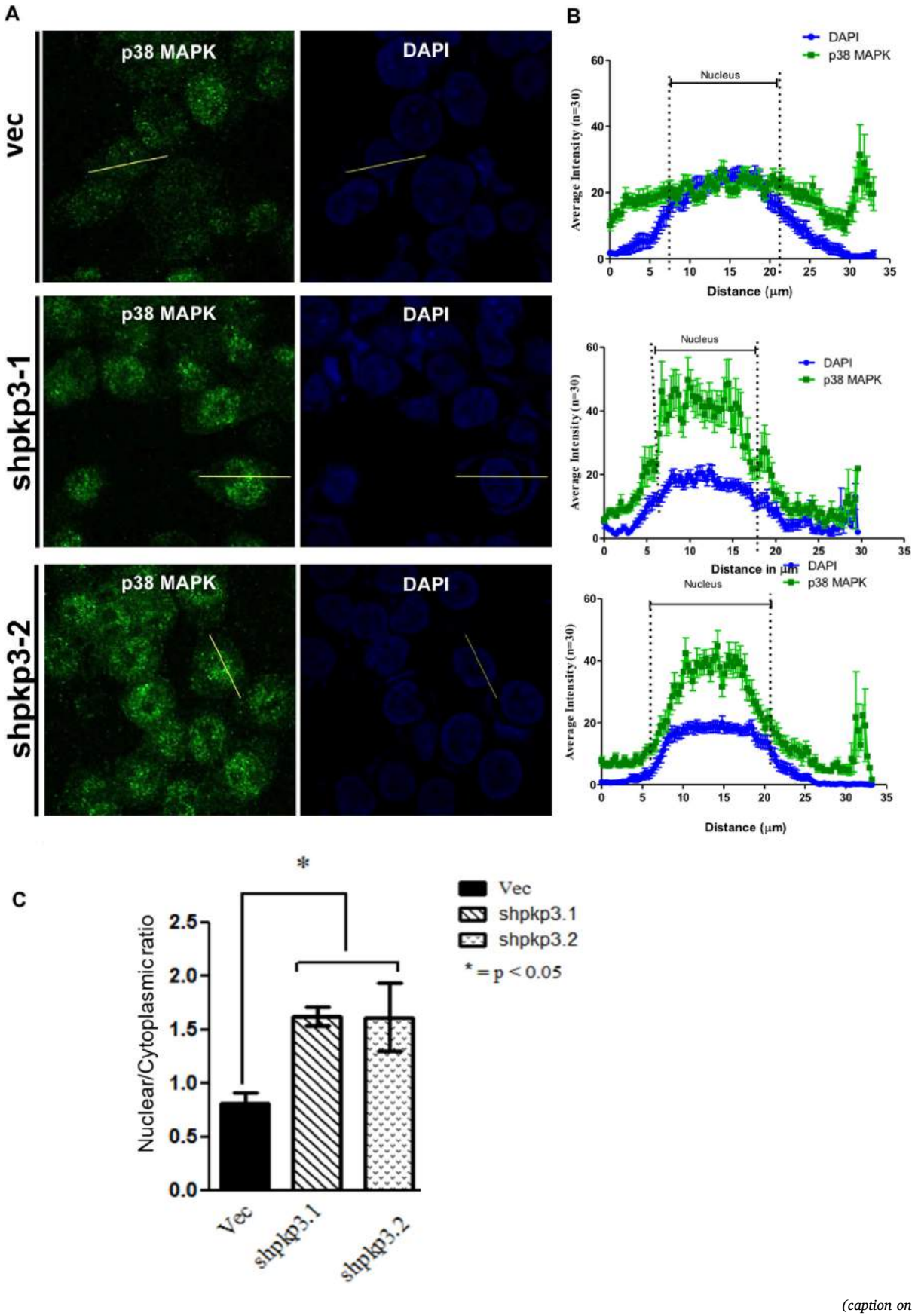

(caption on next page)

Fig. 3. Loss of PKP3 leads to increased nuclear localization of p38. (A) Immuno-fluorescence for p38 MAPK was performed on HCT116 derived vector control and PKP3 knockdown clones. Images were taken using a confocal microscope and representative images are shown. Traces for the green signal and DAPI for the indicated cells are shown. Note that p38 MAPK accumulates in the nucleus in the PKP3 knockdown clones. Scale bars correspond to 10 μm. (B) Intensity profiles of p38MAPK (green) and DAPI (blue) were generated by using line scans drawn across the longest length of 30 random cells in three independent experiments. The average intensity was plotted against the distance (μm), Error bars indicate standard deviation. (C) Immuno-fluorescence for p38 MAPK was performed on HCT116 derived vector control cells and PKP3 knockdown cells, intensity of p38 MAPK in the nucleus and total p38 MAPK was quantitated for 20 random cells in three independent experiments. The ratio of p38 MAPK intensity in the nucleus to the cytoplasm has been plotted. Where indicated the p value was calculated using a student's *t*-test (* indicates p value < 0.05 and n.s indicates non-significant difference).

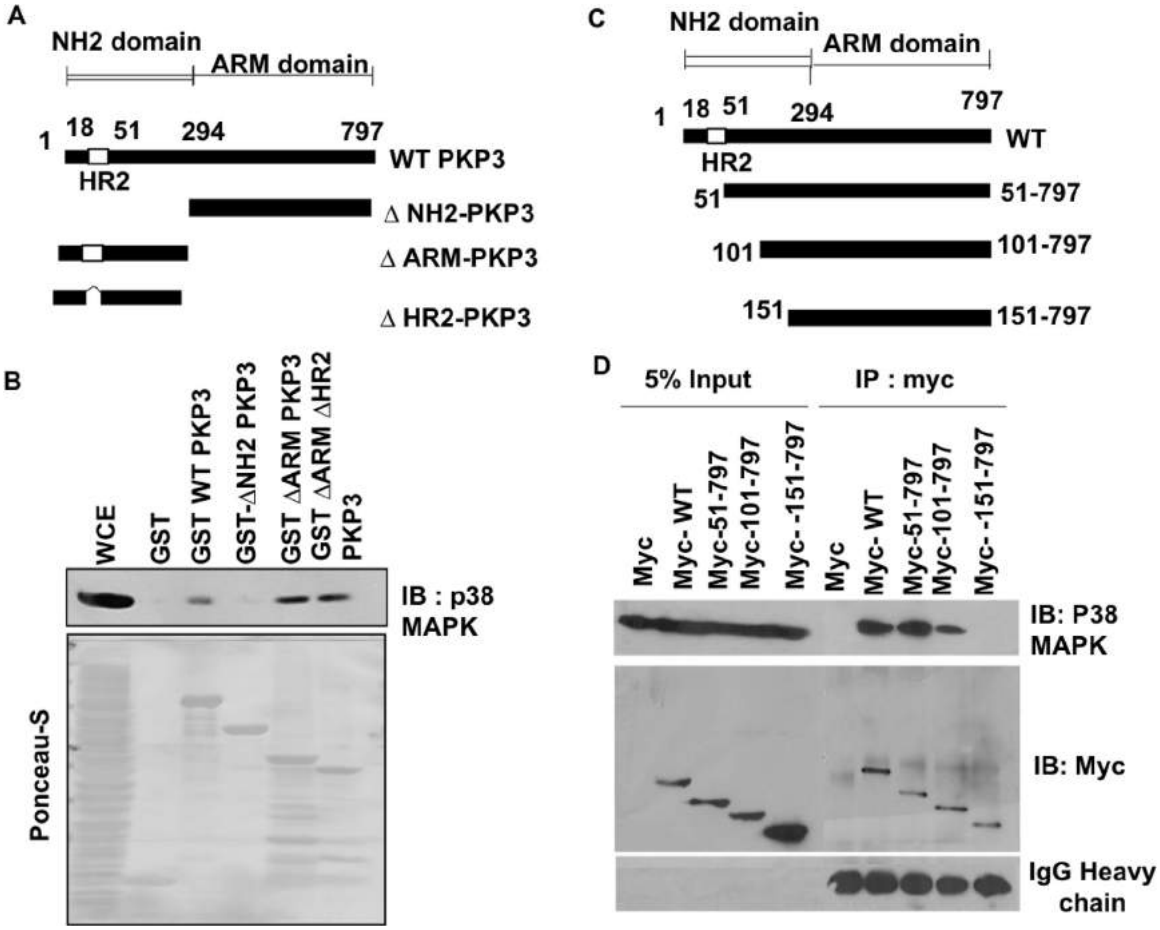

Fig. 4. PKP3 binds to p38 MAPK and restricts p38 MAPK to the cytoplasm. (A) A schematic representation of the PKP3 deletion constructs. The wild type (WT), the N terminal deleted PKP3 (ΔNH2 PKP3), the ARM region deleted PKP3 (ΔARM PKP3) and the Homology region-2 deleted PKP3 (ΔHR2 PKP3) with the respective amino acids in each have been indicated. **(B)** Bacterially expressed, GST fused WT PKP3 or deletion mutants of PKP3 (as indicated) were incubated overnight with protein extracts prepared from HCT116 cells. The GST bound complexes were resolved on SDS-PAGE gels followed by Western blots with antibodies to p38 MAPK (upper panel). The same blot was stained with Ponceau stain to demonstrate equal loading of proteins and molecular sizes of the PKP3 deletion mutants (lower panels). **(C)** Schematic representation of the WT PKP3 and the sequential deletion mutants of the N terminal region of PKP3 named based on their amino acid positions as 51-797, 101-797 and 151-797. **(D)** Myc tagged WT PKP3 or the indicated deletion mutant constructs (Myc-51-797, Myc-101-797 and Myc-151-797) were transfected into HCT116 cells and immunoprecipitations performed with antibodies against the Myc epitope. 5% of the input extract and the immunoprecipitated complexes were resolved on a 10% SDS PAGE gel, and a Western blot analysis performed using antibodies against the Myc epitope or against p38 MAPK as indicated. The heavy chain of the immunoprecipitated myc antibody has been used as a control for the amount of antibody used in each reaction.

experiments suggest that p38β specifically is required for the increase in LCN2 expression observed upon PKP3 loss in HCT116 cells.

4. Discussion

The results presented in this report suggest that LCN2 is required for the tumour progression observed upon PKP3 loss. The increase in LCN2 expression upon PKP3 loss requires an increase in p38 MAPK signalling. Inhibition of p38MAPK activity leads to a decrease in LCN2 expression suggesting that p38β MAPK and not p38α MAPK is required for the increased LCN2 expression observed upon PKP3 loss. Thus, LCN2 might serve as a target for therapeutic intervention in tumours with an increase in LCN2 expression.

In HCT116 cells, loss of PKP3 led to increased tumour formation and metastasis [11]. While PKP3 loss is observed in multiple tumour types and is often associated with increased tumour progression [6,7,9,10], an increase in PKP3 expression is associated with neoplastic progression in a distinct set of tumour types [8,44]. Thus, PKP3 may act as a tumour suppressor or an oncogene in different cell types depending on the context in which PKP3 expression is gained or lost [3]. Multiple studies have demonstrated that increased levels of LCN2 correlated with tumour stage, tumour recurrence and decreased patient survival [19,20,45,46]. Similarly, many reports have suggested that an increase in LCN2 expression can lead to tumour progression in mouse models of

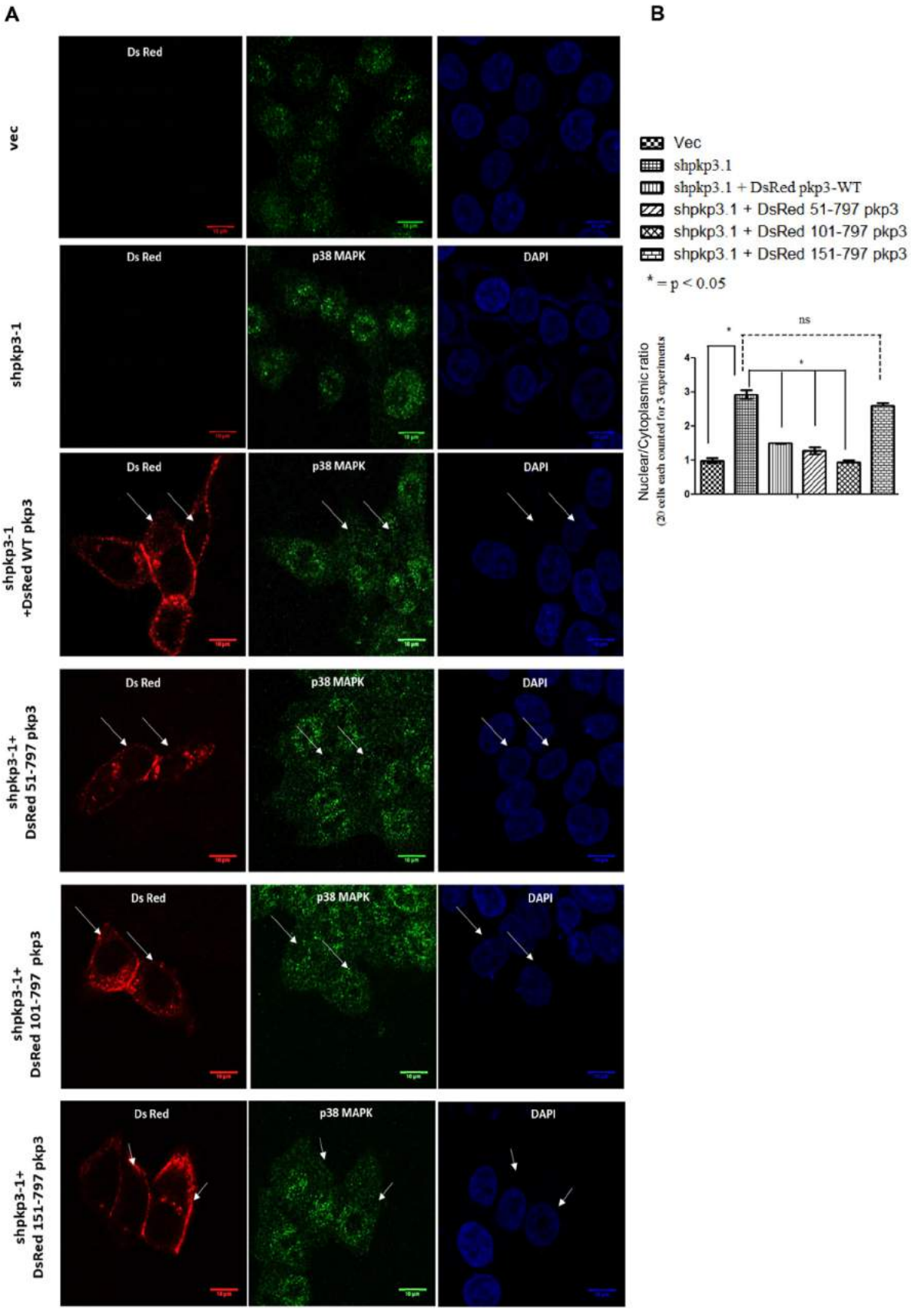

(caption on next page)

Fig. 5. (A) Ds-Red tagged shRNA resistant WT PKP3 or the indicated shRNA resistant deletion mutant constructs of PKP3 were transiently transfected in the PKP3 knockdown clone, shpkp3-1. As controls, the un-transfected PKP3 knockdown clone, shpkp3-1 and the vector control clone, vec cells were used. At 40 h, post transfection, cells were fixed and immunofluorescence was performed using antibody specific to p38 MAPK. The Ds-Red signal was used to identify transfected cells. The white arrows indicate cells expressing Ds-Red tagged WT PKP3 or the deletion mutants of PKP3. Note that expression of Ds-Red WT PKP3 or the Ds-Red shRNA resistant PKP3 mutants 51-797 and 101-797, in the PKP3 knockdown clone shpkp3-1, leads to a decrease in the levels of nuclear p38 MAPK localization, while in cells expressing the PKP3 mutant 151-797, the nuclear levels of p38 MAPK are similar to un-transfected cells. Also, note that nuclear p38 MAPK is higher in PKP3 knockdown clone shpkp3-1 as compared to the vector control clone, vec. Scale bars correspond to 10 μm. **(B)** Immuno-fluorescence for p38 MAPK was performed on HCT116 derived PKP3 knockdown clones transfected with Ds-Red tagged shRNA resistant WT PKP3 or the indicated shRNA resistant deletion mutant constructs of PKP3. For Ds-Red tagged WT or mutant PKP3 transfected cells, intensity of p38 MAPK in the nucleus and total p38 MAPK was quantitated for 20 Ds-Red tagged cells in three independent experiments using ImageJ software. For the un-transfected HCT116 derived vector control cells and PKP3 knockdown cells, intensity of p38 MAPK in the nucleus and total p38 MAPK was quantitated for 20 random cells in three independent experiments. The ratio p38 MAPK intensity in the nucleus to the cytoplasm has been plotted. Where indicated the p value was calculated using a student's *t*-test (* indicates p value < 0.05 and n.s indicates non-significant difference).

breast cancer [47,48] and pancreatic cancer [49]. Higher plasma levels of secreted LCN2 were observed in patients suffering from colorectal cancer and LCN2 levels correlated with increased tumour volume, higher metastasis, shorter disease-free survival and higher recurrence [50]. Consistent with these reports, the results in this report demonstrate that increase in LCN2 expression upon PKP3 loss in HCT116 cells is necessary for cell migration, invasion and anchorage independent growth in vitro and tumour formation in vivo. Since LCN2 knockdown led to a decrease in tumour incidence, the role of LCN2 in the metastasis induced upon PKP3 loss could not be confirmed. As PKP3 loss [6,7,9,10] and LCN2 over-expression [19,20,45,46] are often associated with advanced disease, LCN2 might serve as a marker to identify difficult to treat tumours.

Analysis of a microarray dataset (GSE39582) demonstrated that

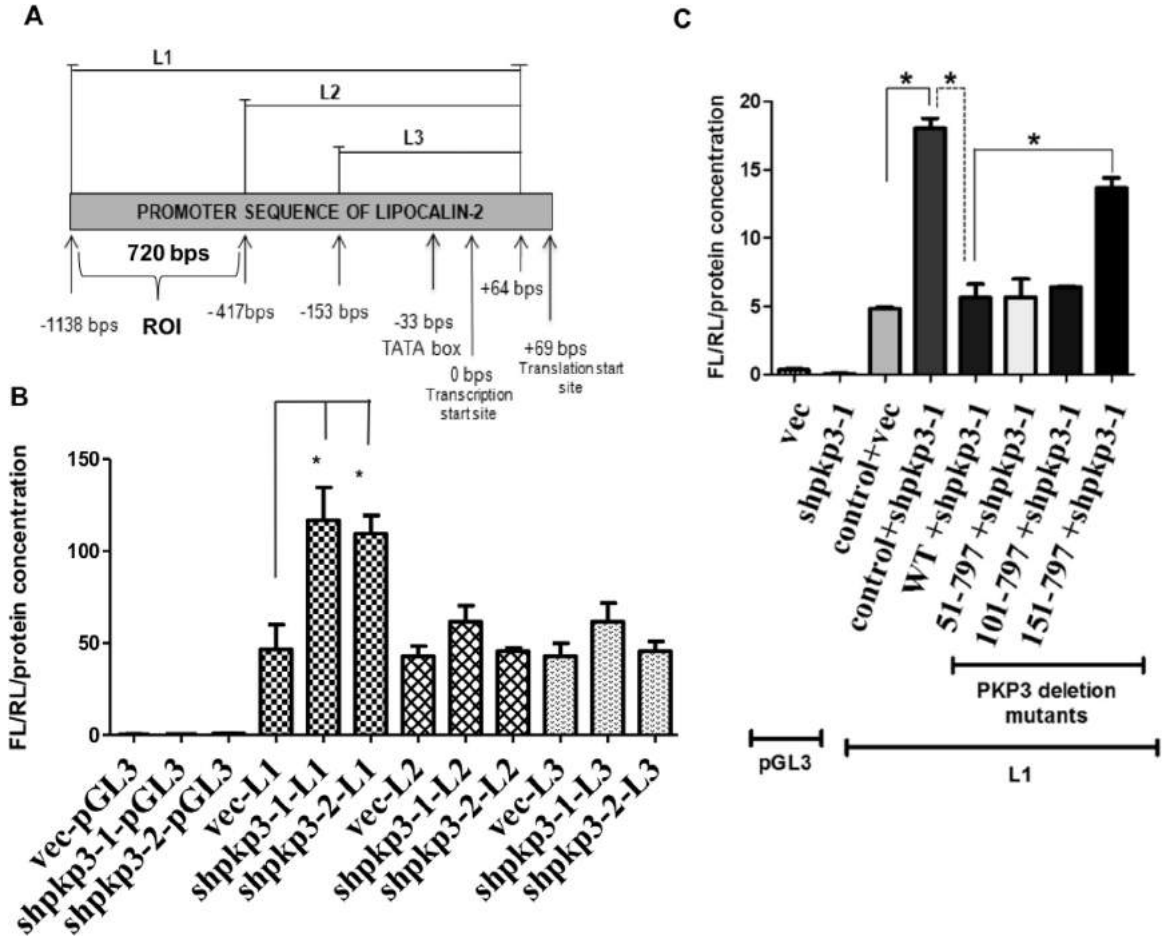

Fig. 6. Complex formation between PKP3 and p38 is required to regulate the expression of LCN2. (A) Schematic representation of the overlapping promoter fragments (L1, L2 and L3) of the LCN2 promoter which were cloned in pGL3 vector (encodes firefly luciferase). The +ve or −ve sign indicates the position of the nucleotide base relative to the transcription start site (TSS) which has been denoted as 0. The translation start site is at position + 69 relative to TSS. The location of the promoter fragments on the LCN2 promoter has been indicated in base pairs. **(B)** The vector control and PKP3 knockdown clones were transfected with the indicated firefly luciferase (FL) reporter plasmids and a renilla luciferase (RL) expressing plasmid (pRL TK), which served as a transfection control. The ratio of FL/RL/protein concentration of the different promoter constructs has been plotted on the Y axis. The mean and standard error of three independent experiments is plotted. **(C)** The LCN2 promoter driven luciferase reporter vector L1 was transiently transfected along with Ds-Red tagged shRNA resistant WT PKP3 or the indicated deletion mutants of PKP3 (51-797, 101-797 and 151-797) in the HCT116 derived PKP3 knockdown clone shpkp3-1 or the vector control clone, vec. As controls, the L1 construct was transfected in the clones, shpkp3-1 and vec, along with the control vector (pcDNA3). The Renilla luciferase containing vector pRL-TK was also transiently transfected and acted as a transfection control for the experiment. Luciferase reporter assays were performed and the ratio of FL/RL/protein concentration in the corresponding cells has been plotted on Y axis. The p value was calculated using a student's *t*-test and plotted (* indicates p value < 0.01).

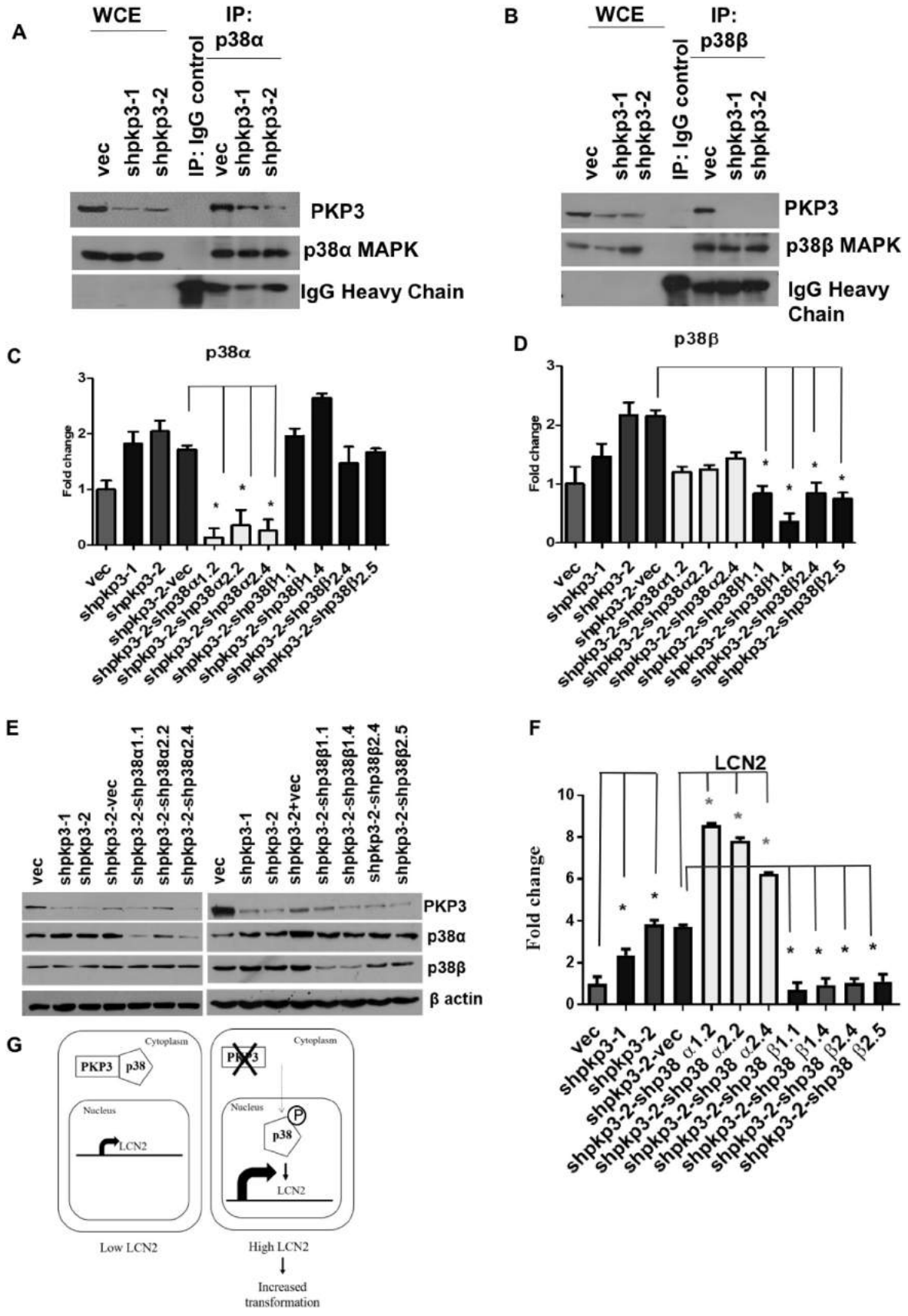

(caption on next page)

Fig. 7. PKP3 binds to both p38α and p38β MAPK but only p38β MAPK activation is required for increase in LCN2 expression upon PKP3 loss (A–B) Whole cell extracts were prepared from HCT116 derived PKP3 knockdown and vector control clones and immunoprecipitation experiments were performed using p38α MAPK antibody (A) or p38β MAPK antibody (B). The immunoprecipitated samples along with 5% input of the whole cell extracts (collected before immunoprecipitation) were run on 7.5% SDS PAGE gel followed by Western blotting with antibodies against PKP3 and either p38α MAPK **(A)** or p38β MAPK **(B)**. The heavy chain of the antibody used for immunoprecipitation has been indicated. Note that PKP3 co-precipitates with both p38α and p38β and that this is decreased in PKP3 knockdown cells**. (C–D)** Real time PCRs were performed using oligonucleotides specific for p38α MAPK **(C)** or p38β MAPK **(D)** and GAPDH in HCT116 derived PKP3 knockdown clones (shpkp3-1 and shpkp3-2), its vector control clone (vec), the shpkp3-2 derived p38α + PKP3 double knockdown clones and shpkp3-2 derived p38β + PKP3 double knockdown clones. **(E)** 75 μg of a whole cell extract obtained from the HCT116 derived PKP3 knockdown clones, the vector control clone (vec), the PKP3 knockdown clones (shpkp3-1 and shpkp3-2), the p38α + PKP3 double knockdown clones (shpkp3-2-shp38α1.1, shpkp3-2-shp38α2.2 and shpkp3-2-shp38α2.4), the p38β + PKP3 double knockdown clones (shpkp3-2-shp38β1.1, shpkp3-2-shp38β1.4, shpkp3-2-shp38β2.4 and shpkp3-2-shp38β2.5) and the shpkp3-2 derived vector control clone (shpkp3-2-vec) were resolved on 10% SDS PAGE gels followed by Western blotting with antibodies specific to PKP3, p38α MAPK, p38β MAPK and β actin (loading control). Note that in the p38α + PKP3 double knockdown clones, p38α expression decreases and p38β remains unaltered, while in the p38β + PKP3 double knockdown clones, p38β decreases while p38α levels remain unaltered. **(F)** Real time PCRs were performed using oligonucleotides specific for LCN2 and GAPDH (for normalization), in PKP3 knockdown clones, its vector control, the p38α + PKP3 double knockdown clones, the p38β + PKP3 double knockdown clones and the respective vector control clone. The fold change in LCN2 mRNA was measured. The mean values and standard errors are plotted. Where indicated the p value was calculated using a student's *t*-test (* indicates p value < 0.01). **(G)** Proposed model for increase in LCN2 expression upon PKP3 knockdown in HCT116 cells.

LCN2 expression was high and PKP3 expression low in colon cancer patients as compared to normal controls. An in-silico analysis demonstrated that in > 59% of the samples with low expression of PKP3 showed high LCN2 levels (Fig. S2B–C). While all the samples with PKP3 loss do not show an increase in LCN2 expression, the data suggest that a significant percentage of the tumour samples do show an increase in LCN2 expression upon PKP3 loss. This suggests that a detailed analysis of PKP3 and LCN2 protein levels needs to be performed in a large cohort of colon cancer patients with the adjacent normal tissues from the same patients serving as controls, to determine whether this complex signalling pathway plays a role in tumorigenesis and metastasis and should be accompanied by a detailed survival analysis of these patients to determine if PKP3 or LCN2 expression correlates with either overall survival or disease-free survival.

In cancers such as breast cancer [51] and bladder cancer [52], the effect of LCN2 on tumour formation depends on its ability to form a complex with MMP9 and prevent the degradation of MMP9 by other proteases thus increasing protein stability and activity of MMP9 [53]. Unlike breast cancers or bladder cancers, LCN2 serves as an independent prognostic marker for colon cancers as its effect on neoplastic progression was shown to be independent of MMP9 activity [46,54]. Consistent with these reports, results presented in this paper demonstrate that the effect of LCN2 in increasing neoplastic progression upon PKP3 loss in HCT116 cells is independent of MMP9 levels or activity because HCT116 cells do not express MMP9 mRNA [12].

Previous reports suggest that activation of the p38 MAPK and ERK1/2 pathways led to an increase in LCN2 expression in intestinal epithelial cells [30]. PKP3 loss in HCT116 cells leads to a decrease in desmosome formation [11,22,55] and activation of p38 MAPK (this report), which are consistent with reports demonstrating that a disruption of desmosome structure leads to p38 MAPK activation [33–35]. Inhibition of p38 activity has been shown to decrease disease progression induced by the pemphigus vulgaris (PV) antibodies [33–35] and the loss of another plakophilin family member, PKP2, results in the activation of p38 signalling in cardiomyocytes [56]. The results in this report suggest that PKP3 physically forms a complex with p38 and inhibits the transport of p38 to the nucleus thereby affecting gene expression. Previous reports have demonstrated that in addition to being present at the cell border, PKP3 is also found in cytoplasmic granules [57–59]. We have not observed any co-localization between p38 and PKP3 either at the cell border or in the cytoplasm. Therefore, the inhibition of p38 localization by PKP3 might be independent of the ability of p38 MAPK to localize to the desmosome and might be another cytoplasmic function of PKP3 in addition to those previously reported [58].

Although, p38 MAPK activation can increase LCN2 expression [29,30], this is the first report that identifies the p38 isoform required for LCN2 expression. Our results demonstrate that p38α and p38β might play opposing roles in regulating LCN2 expression and the balance between the activities of these two isoforms may be one of the mechanisms by which p38 MAPKs regulate tumour progression. In agreement with this hypothesis, p38α functions as a tumour suppressor role in colon cancers [60] and knocking down p38α increases tumour formation in axoxymethane (AOM)-DSS induced inflammation associated colon cancers [61]. These results are consistent with our observations that p38α might inhibit the transcription of LCN2. The specific role of p38β in colon cancers has not been elucidated though our results would suggest that activation of p38β might lead to an increase in tumour formation.

The results of this report demonstrate that PKP3 associates with both p38α and p38β. The p38 binding site in PKP3 maps to the 151-797 amino acid region of PKP3. PKP3 loss leads to increased nuclear translocation of p38 MAPK thus leading to an increase in LCN2 transcription and re-expression of PKP3 leads to the increased localization of p38 to the cytoplasm and a decrease in LCN2 expression. In addition, the fractionation data suggests that most of the activated p38 MAPK is present in the nucleus suggesting that disruption of the PKP3 p38 complex might lead to the activation and nuclear translocation of p38. These results suggest that one possible mechanism by which PKP3 might regulate p38 function is by retaining it in the cytoplasm and preventing it from accessing its nuclear substrates or transcription factors. These data are consistent with earlier reports that desmosomal proteins (like DSG3) associate with p38 MAPK and loss or disruption of desmosomal proteins may lead to changes in p38 MAPK signalling [62–65]. These results suggest that cytoplasmic PKP3 in addition to its previously reported role in regulating translation [57,66] might have other functions such as inhibiting the transport of p38 MAPK to the nucleus.

The results in this report allow us to generate the following model (Fig. 7G). PKP3 forms a complex with p38MAPK resulting in the retention of p38MAPK in the cytoplasm. Whether PKP3 or another protein complex is required for the sequestration of p38 is not clear as we were unable to determine if p38 and PKP3 co-localized in the cytoplasm. PKP3 loss leads to activation of and nuclear transport of p38 MAPK, which is required for the increase in LCN2 observed upon PKP3 loss. While our results suggest that the p38β isoform is required for the increase in LCN2 expression and tumour progression, both p38α and p38β form a complex with PKP3 and we cannot rule out the possibility that p38α has a role to play in the transformation induced by PKP3 loss. Alternatively, the association of PKP3 with p38α might be required for the regulation of desmosome formation by PKP3 and not for the increased transformation and tumour progression observed upon PKP3 loss. As the increase in LCN2 expression is required for the increased migration, invasion, transformation and tumour progression observed upon PKP3 loss, LCN2 might serve as a target for therapeutic intervention in epithelial tumours.

5. Conclusions

This report demonstrates that LCN2 expression is increased upon PKP3 loss via p38β MAPK signalling and that LCN2 is required for increased tumour formation upon PKP3 loss. LCN2 may serve as a predictive marker for locally advanced disease.

Acknowledgements

This work was supported by a grant from the Department of Science and Technology, Govt. of India (Grant no. SR/SO/HS-011/2009) and funds from ACTREC 42. S.B. was supported by fellowships from the Council for Scientific and Industrial Research 20-6/2008(ii) EU-IV and the Department of Biotechnology BT/PR8351/MED/30/995/2013. We thank the ACTREC microscopy facility for help with acquisition of images used in this report. We thank Drs. S. Bonne and F. van Roy for the myc tagged plakophilin3 construct.

Appendix A. Supplementary material

Supplementary data associated with this article can be found in the online version at http://dx.doi.org/10.1016/j.yexcr.2018.05.026.

References

[1] B.V. Desai, R.M. Harmon, K.J. Green, Desmosomes at a glance, J. Cell Sci. 122 (2009) 4401–4407.
[2] D.R. Garrod, A.J. Merritt, Z. Nie, Desmosomal adhesion: structural basis, molecular mechanism and regulation (review), Mol. Membr. Biol. 19 (2002) 81–94.
[3] S. Neuber, M. Muhmer, D. Wratten, P.J. Koch, R. Moll, A. Schmidt, The desmosomal plaque proteins of the plakophilin family, Dermatol. Res. Pract. 2010 (2010) 101452.
[4] S. Bonne, B. Gilbert, M. Hatzfeld, X. Chen, K.J. Green, F. van Roy, Defining desmosomal plakophilin-3 interactions, J. Cell Biol. 161 (2003) 403–416.
[5] B.J. Roberts, R. Reddy, J.K. Wahl 3rd, Stratifin (14-3-3 sigma) limits plakophilin-3 exchange with the desmosomal plaque, PLoS One 8 (2013) e77012.
[6] K. Aigner, L. Descovich, M. Mikula, A. Sultan, B. Dampier, S. Bonne, F. van Roy, W. Mikulits, M. Schreiber, T. Brabletz, W. Sommergruber, N. Schweifer, A. Wernitznig, H. Beug, R. Foisner, A. Eger, The transcription factor ZEB1 (deltaEF1) represses plakophilin 3 during human cancer progression, FEBS Lett. 581 (2007) 1617–1624.
[7] G.G. Demirag, Y. Sullu, D. Gurgenyatagi, N.O. Okumus, I. Yucel, Expression of plakophilins (PKP1, PKP2, and PKP3) in gastric cancers, Diagn. Pathol. 6 (2011) 1.
[8] G.G. Demirag, Y. Sullu, I. Yucel, Expression of plakophilins (PKP1, PKP2, and PKP3) in breast cancers, Med. Oncol. 29 (2012) 1518–1522.
[9] S. Papagerakis, A.H. Shabana, J. Depondt, P. Gehanno, N. Forest, Immunohistochemical localization of plakophilins (PKP1, PKP2, PKP3, andp0071) in primary oropharyngeal tumors: correlation with clinical parameters, Hum. Pathol. 34 (2003) 565–572.
[10] H. Takahashi, H. Nakatsuji, M. Takahashi, S. Avirmed, T. Fukawa, M. Takemura, T. Fukumori, H. Kanayama, Up-regulation of plakophilin-2 and down-regulation of plakophilin-3 are correlated with invasiveness in bladder cancer, Urology 79 (2012) e241–e248 (240).
[11] S.T. Kundu, P. Gosavi, N. Khapare, R. Patel, A.S. Hosing, G.B. Maru, A. Ingle, J.A. Decaprio, S.N. Dalal, Plakophilin3 downregulation leads to a decrease in cell adhesion and promotes metastasis, Int. J. Cancer 123 (2008) 2303–2314.
[12] S. Basu, R. Thorat, S.N. Dalal, MMP7 is required to mediate cell invasion and tumor formation upon plakophilin3 loss, PLoS One 10 (2015) e0123979.
[13] N. Khapare, S.T. Kundu, L. Sehgal, M. Sawant, R. Priya, P. Gosavi, N. Gupta, H. Alam, M. Karkhanis, N. Naik, M.M. Vaidya, S.N. Dalal, Plakophilin3 loss leads to an increase in PRL3 levels promoting K8 dephosphorylation, which is required for transformation and metastasis, PLoS One 7 (2012) e38561.
[14] S. Chakraborty, S. Kaur, S. Guha, S.K. Batra, The multifaceted roles of neutrophil gelatinase associated lipocalin (NGAL) in inflammation and cancer, Biochim. Biophys. Acta 1826 (2012) 129–169.
[15] K.M. Schmidt-Ott, K. Mori, A. Kalandadze, J.Y. Li, N. Paragas, T. Nicholas, P. Devarajan, J. Barasch, Neutrophil gelatinase-associated lipocalin-mediated iron traffic in kidney epithelia, Curr. Opin. Nephrol. Hypertens. 15 (2006) 442–449.
[16] R.J. Playford, A. Belo, R. Poulsom, A.J. Fitzgerald, K. Harris, I. Pawluczyk, J. Ryon, T. Darby, M. Nilsen-Hamilton, S. Ghosh, T. Marchbank, Effects of mouse and human lipocalin homologues 24p3/lcn2 and neutrophil gelatinase-associated lipocalin on gastrointestinal mucosal integrity and repair, Gastroenterology 131 (2006) 809–817.
[17] J.J. Rodvold, N.R. Mahadevan, M. Zanetti, Lipocalin 2 in cancer: when good immunity goes bad, Cancer Lett. 316 (2012) 132–138.
[18] B.S. Nielsen, N. Borregaard, J.R. Bundgaard, S. Timshel, M. Sehested, L. Kjeldsen, Induction of NGAL synthesis in epithelial cells of human colorectal neoplasia and inflammatory bowel diseases, Gut 38 (1996) 414–420.
[19] Y. Sun, K. Yokoi, H. Li, J. Gao, L. Hu, B. Liu, K. Chen, S.R. Hamilton, D. Fan, B. Sun, W. Zhang, NGAL expression is elevated in both colorectal adenoma-carcinoma sequence and cancer progression and enhances tumorigenesis in xenograft mouse models, Clin. Cancer Res. 17 (2011) 4331–4340.
[20] M.H. McLean, A.J. Thomson, G.I. Murray, N. Fyfe, G.L. Hold, E.M. El-Omar, Expression of neutrophil gelatinase-associated lipocalin in colorectal neoplastic progression: a marker of malignant potential? Br. J. Cancer 108 (2013) 2537–2541.
[21] L. Sehgal, R. Thorat, N. Khapare, A. Mukhopadhaya, M. Sawant, S.N. Dalal, Lentiviral mediated transgenesis by in vivo manipulation of spermatogonial stem cells, PLoS One 6 (2011) e21975.
[22] P. Gosavi, S.T. Kundu, N. Khapare, L. Sehgal, M.S. Karkhanis, S.N. Dalal, E-cadherin and plakoglobin recruit plakophilin3 to the cell border to initiate desmosome assembly, Cell. Mol. Life Sci. 68 (2011) 1439–1454.
[23] U. Raul, S. Sawant, P. Dange, R. Kalraiya, A. Ingle, M. Vaidya, Implications of cytokeratin 8/18 filament formation in stratified epithelial cells: induction of transformed phenotype, Int. J. Cancer 111 (2004) 662–668.
[24] C.J. Liao, P.T. Li, Y.C. Lee, S.H. Li, S.T. Chu, Lipocalin 2 induces the epithelial-mesenchymal transition in stressed endometrial epithelial cells: possible correlation with endometriosis development in a mouse model, Reproduction 147 (2014) 179–187.
[25] A. Kondo, S. Yamamoto, R. Nakaki, T. Shimamura, T. Hamakubo, J. Sakai, T. Kodama, T. Yoshida, H. Aburatani, T. Osawa, Extracellular acidic pH activates the sterol regulatory element-binding protein 2 to promote tumor progression, Cell Rep. 18 (2017) 2228–2242.
[26] N.R. Mahadevan, J. Rodvold, G. Almanza, A.F. Perez, M.C. Wheeler, M. Zanetti, ER stress drives Lipocalin 2 upregulation in prostate cancer cells in an NF-kappaB-dependent manner, BMC Cancer 11 (2011) 229.
[27] S.N. Dalal, C.M. Schweitzer, J. Gan, J.A. DeCaprio, Cytoplasmic localization of human cdc25C during interphase requires an intact 14-3-3 binding site, Mol. Cell. Biol. 19 (1999) 4465–4479.
[28] C. Zer, G. Sachs, J.M. Shin, Identification of genomic targets downstream of p38 mitogen-activated protein kinase pathway mediating tumor necrosis factor-alpha signaling, Physiol. Genom. 31 (2007) 343–351.
[29] L.H. Wang, G.Q. Chang, H.J. Zhang, J. Wang, Y.N. Lin, W.N. Jin, H.W. Li, W. Gao, R.J. Wang, Q.H. Li, T.X. Pang, Neutrophil gelatinase-associated lipocalin regulates intracellular accumulation of Rh123 in cancer cells, Genes Cells 17 (2012) 205–217.
[30] Y. Yoo do, S.H. Ko, J. Jung, Y.J. Kim, J.S. Kim, J.M. Kim, Bacteroides fragilis enterotoxin upregulates lipocalin-2 expression in intestinal epithelial cells, Lab. Invest. 93 (2013) 384–396.
[31] E.R. Butch, K.L. Guan, Characterization of ERK1 activation site mutants and the effect on recognition by MEK1 and MEK2, J. Biol. Chem. 271 (1996) 4230–4235.
[32] Y.Y. Zhang, Z.Q. Mei, J.W. Wu, Z.X. Wang, Enzymatic activity and substrate specificity of mitogen-activated protein kinase p38alpha in different phosphorylation states, J. Biol. Chem. 283 (2008) 26591–26601.
[33] P. Berkowitz, P. Hu, Z. Liu, L.A. Diaz, J.J. Enghild, M.P. Chua, D.S. Rubenstein, Desmosome signaling. Inhibition of p38MAPK prevents pemphigus vulgaris IgG-induced cytoskeleton reorganization, J. Biol. Chem. 280 (2005) 23778–23784.
[34] P. Berkowitz, P. Hu, S. Warren, Z. Liu, L.A. Diaz, D.S. Rubenstein, p38MAPK inhibition prevents disease in pemphigus vulgaris mice, Proc. Natl. Acad. Sci. USA 103 (2006) 12855–12860.
[35] V. Rotzer, E. Hartlieb, F. Vielmuth, M. Gliem, V. Spindler, J. Waschke, E-cadherin and Src associate with extradesmosomal Dsg3 and modulate desmosome assembly and adhesion, Cell. Mol. Life Sci. 72 (2015) 4885–4897.
[36] R.J. Gum, M.M. McLaughlin, S. Kumar, Z. Wang, M.J. Bower, J.C. Lee, J.L. Adams, G.P. Livi, E.J. Goldsmith, P.R. Young, Acquisition of sensitivity of stress-activated protein kinases to the p38 inhibitor, SB 203580, by alteration of one or more amino acids within the ATP binding pocket, J. Biol. Chem. 273 (1998) 15605–15610.
[37] S. Kumar, P.C. McDonnell, R.J. Gum, A.T. Hand, J.C. Lee, P.R. Young, Novel homologues of CSBP/p38 MAP kinase: activation, substrate specificity and sensitivity to inhibition by pyridinyl imidazoles, Biochem. Biophys. Res. Commun. 235 (1997) 533–538.
[38] X. Gong, X. Ming, P. Deng, Y. Jiang, Mechanisms regulating the nuclear translocation of p38 MAP kinase, J. Cell. Biochem. 110 (2010) 1420–1429.
[39] L. Wang, H. Li, J. Wang, W. Gao, Y. Lin, W. Jin, G. Chang, R. Wang, Q. Li, L. Ma, T. Pang, C/EBP zeta targets to neutrophil gelatinase-associated lipocalin (NGAL) as a repressor for metastasis of MDA-MB-231 cells, Biochim. Biophys. Acta 1813 (2011) 1803–1813.
[40] J.B. Cowland, N. Borregaard, Molecular characterization and pattern of tissue expression of the gene for neutrophil gelatinase-associated lipocalin from humans, Genomics 45 (1997) 17–23.
[41] W.W. Lorenz, R.O. McCann, M. Longiaru, M.J. Cormier, Isolation and expression of a cDNA encoding Renilla reniformis luciferase, Proc. Natl. Acad. Sci. USA 88 (1991) 4438–4442.
[42] R.C. Hart, J.C. Matthews, K. Hori, M.J. Cormier, Renilla reniformis bioluminescence: luciferase-catalyzed production of nonradiating excited states from luciferin analogues and elucidation of the excited state species involved in energy transfer to Renilla green fluorescent protein, Biochemistry 18 (1979) 2204–2210.
[43] Y. Jiang, C. Chen, Z. Li, W. Guo, J.A. Gegner, S. Lin, J. Han, Characterization of the structure and function of a new mitogen-activated protein kinase (p38beta), J. Biol. Chem. 271 (1996) 17920–17926.
[44] C. Furukawa, Y. Daigo, N. Ishikawa, T. Kato, T. Ito, E. Tsuchiya, S. Sone, Y. Nakamura, Plakophilin 3 oncogene as prognostic marker and therapeutic target for lung cancer, Cancer Res 65 (2005) 7102–7110.
[45] V. Barresi, C. Di Gregorio, L. Reggiani-Bonetti, A. Ieni, M. Ponz-De Leon, G. Barresi, Neutrophil gelatinase-associated lipocalin: a new prognostic marker in stage I

colorectal carcinoma? Hum. Pathol. 42 (2011) 1720–1726.
[46] V. Barresi, L. Reggiani-Bonetti, C. Di Gregorio, E. Vitarelli, M. Ponz De Leon, G. Barresi, Neutrophil gelatinase-associated lipocalin (NGAL) and matrix metalloproteinase-9 (MMP-9) prognostic value in stage I colorectal carcinoma, Pathol. Res. Pract. 207 (2011) 479–486.
[47] T. Berger, C.C. Cheung, A.J. Elia, T.W. Mak, Disruption of the Lcn2 gene in mice suppresses primary mammary tumor formation but does not decrease lung metastasis, Proc. Natl. Acad. Sci. USA 107 (2010) 2995–3000.
[48] X. Leng, T. Ding, H. Lin, Y. Wang, L. Hu, J. Hu, B. Feig, W. Zhang, L. Pusztai, W.F. Symmans, Y. Wu, R.B. Arlinghaus, Inhibition of lipocalin 2 impairs breast tumorigenesis and metastasis, Cancer Res. 69 (2009) 8579–8584.
[49] S.B. Gomez-Chou, A.K. Swidnicka-Siergiejko, N. Badi, M. Chavez-Tomar, G.B. Lesinski, T. Bekaii-Saab, M.R. Farren, T.A. Mace, C. Schmidt, Y. Liu, D. Deng, R.F. Hwang, L. Zhou, T. Moore, D. Chatterjee, H. Wang, X. Leng, R.B. Arlinghaus, C.D. Logsdon, Z. Cruz-Monserrate, Lipocalin-2 promotes pancreatic ductal adenocarcinoma by regulating inflammation in the tumor microenvironment, Cancer Res. 77 (2017) 2647–2660.
[50] J. Marti, J. Fuster, A.M. Sola, G. Hotter, R. Molina, A. Pelegrina, J. Ferrer, R. Deulofeu, C. Fondevila, J.C. Garcia-Valdecasas, Prognostic value of serum neutrophil gelatinase-associated lipocalin in metastatic and nonmetastatic colorectal cancer, World J. Surg. 37 (2013) 1103–1109.
[51] C.A. Fernandez, L. Yan, G. Louis, J. Yang, J.L. Kutok, M.A. Moses, The matrix metalloproteinase-9/neutrophil gelatinase-associated lipocalin complex plays a role in breast tumor growth and is present in the urine of breast cancer patients, Clin. Cancer Res. 11 (2005) 5390–5395.
[52] F. Monier, A. Surla, M. Guillot, F. Morel, Gelatinase isoforms in urine from bladder cancer patients, Clin. Chim. Acta 299 (2000) 11–23.
[53] L. Yan, N. Borregaard, L. Kjeldsen, M.A. Moses, The high molecular weight urinary matrix metalloproteinase (MMP) activity is a complex of gelatinase B/MMP-9 and neutrophil gelatinase-associated lipocalin (NGAL). Modulation of MMP-9 activity by NGAL, J. Biol. Chem. 276 (2001) 37258–37265.
[54] L. Hu, W. Hittelman, T. Lu, P. Ji, R. Arlinghaus, I. Shmulevich, S.R. Hamilton, W. Zhang, NGAL decreases E-cadherin-mediated cell-cell adhesion and increases cell motility and invasion through Rac1 in colon carcinoma cells, Lab. Invest. 89 (2009) 531–548.
[55] V. Todorovic, J.L. Koetsier, L.M. Godsel, K.J. Green, Plakophilin 3 mediates Rap1-dependent desmosome assembly and adherens junction maturation, Mol. Biol. Cell 25 (2014) 3749–3764.
[56] A.D. Dubash, C.Y. Kam, B.A. Aguado, D.M. Patel, M. Delmar, L.D. Shea, K.J. Green, Plakophilin-2 loss promotes TGF-beta1/p38 MAPK-dependent fibrotic gene expression in cardiomyocytes, J. Cell Biol. 212 (2016) 425–438.
[57] R. Fischer-Keso, S. Breuninger, S. Hofmann, M. Henn, T. Rohrig, P. Strobel, G. Stoecklin, I. Hofmann, Plakophilins 1 and 3 bind to FXR1 and thereby influence the mRNA stability of desmosomal proteins, Mol. Cell. Biol. (2014).
[58] I. Hofmann, M. Casella, M. Schnolzer, T. Schlechter, H. Spring, W.W. Franke, Identification of the junctional plaque protein plakophilin 3 in cytoplasmic particles containing RNA-binding proteins and the recruitment of plakophilins 1 and 3 to stress granules, Mol. Biol. Cell 17 (2006) 1388–1398.
[59] C. Mertens, I. Hofmann, Z. Wang, M. Teichmann, S.S. Chong, M. Schnolzer, W.W. Franke, Nuclear particles containing RNA polymerase III complexes associated with the junctional plaque proteinplakophilin2, Proc. Natl. Acad. Sci. USA 98 (2001) 7795–7800.
[60] D. Wakeman, J.E. Schneider, J. Liu, W.S. Wandu, C.R. Erwin, J. Guo, T.S. Stappenbeck, B.W. Warner, Deletion of p38-alpha mitogen-activated protein kinase within the intestinal epithelium promotes colon tumorigenesis, Surgery 152 (2012) 286–293.
[61] J. Gupta, I. del Barco Barrantes, A. Igea, S. Sakellariou, I.S. Pateras, V.G. Gorgoulis, A.R. Nebreda, Dual function of p38alpha MAPK in colon cancer: suppression of colitis-associated tumor initiation but requirement for cancer cell survival, Cancer Cell 25 (2014) 484–500.
[62] Y. Aoyama, Y. Kitajima, Pemphigus vulgaris-IgG causes a rapid depletion of desmoglein 3 (Dsg3) from the Triton X-100 soluble pools, leading to the formation of Dsg3-depleted desmosomes in a human squamous carcinoma cell line, DJM-1 cells, J. Invest. Dermatol. 112 (1999) 67–71.
[63] C.C. Calkins, S.V. Setzer, J.M. Jennings, S. Summers, K. Tsunoda, M. Amagai, A.P. Kowalczyk, Desmoglein endocytosis and desmosome disassembly are coordinated responses to pemphigus autoantibodies, J. Biol. Chem. 281 (2006) 7623–7634.
[64] M. Amagai, K. Tsunoda, H. Suzuki, K. Nishifuji, S. Koyasu, T. Nishikawa, Use of autoantigen-knockout mice in developing an active autoimmune disease model for pemphigus, J. Clin. Invest. 105 (2000) 625–631.
[65] X. Mao, Y. Sano, J.M. Park, A.S. Payne, p38 MAPK activation is downstream of the loss of intercellular adhesion in pemphigus vulgaris, J. Biol. Chem. 286 (2011) 1283–1291.
[66] C. Yang, P. Strobel, A. Marx, I. Hofmann, Plakophilin-associated RNA-binding proteins in prostate cancer and their implications in tumor progression and metastasis, Virchows Arch. 463 (2013) 379–390.